

Generalized inclusion of short-range ordering effects in the coherent potential approximation for complex-unit-cell materials

Alberto Marmodoro,^{1,2,*} Arthur Ernst,² Sergei Ostanin,² and Julie B. Staunton¹

¹*University of Warwick, Department of Physics, Coventry, CV4 7AL, United Kingdom*

²*Max-Planck-Institut für Mikrostrukturphysik, Weinberg 2, D-06120 Halle, Germany*

(Received 26 June 2012; revised manuscript received 20 December 2012; published 12 March 2013)

The coherent potential approximation has historically allowed the efficient study of disorder effects over a variety of solid state systems. Its original formulation is, however, limited to a single-site or uncorrelated model of local substitutions. This neglects the effects of correlation and short-range ordering, often found in real materials. Recent theoretical work has shown one possible way to systematically address such shortcomings for simple materials with only one element per unit cell. We briefly review the basic ideas of such development within the framework of multiple scattering theory and suggest its generalization to materials with complex lattices. We validate our extension through a systematic comparison with a classic $\text{Cu}_{1-c}\text{Zn}_c$ reference test case and propose, for further illustration of local environment effects, the example of the yttria-stabilized cubic phase of zirconia, re-examined through various techniques for the first-principles treatment of disorder.

DOI: [10.1103/PhysRevB.87.125115](https://doi.org/10.1103/PhysRevB.87.125115)

PACS number(s): 71.23.-k, 71.15.Mb, 71.15.Ap, 71.15.Dx

I. INTRODUCTION

The first-principles treatment of solid state systems in the presence of disorder poses an extra degree of technical and numerical difficulties due to loss of crystalline periodicity.¹ Some deviations from perfect lattice translational invariance are, however, to some extent always present—real samples usually contain various kinds of defects, which may have a significant influence on the fine details of their electronic structure.²

Moreover, the general framework of a substitutional model of disorder, where the occupation of any lattice site by alternative species is only determined in probabilistic terms, applies to a variety of other physical problems of great practical interest. In addition to the study of metallic alloys,^{3–12} this includes, among various examples, doped semiconductors, but also random spin systems¹³ such as magnetic materials above a critical ordering temperature,¹⁴ as well as phonons,^{15–17} and further scenarios from different contexts of condensed matter physics.^{6,18}

One efficient technique to tackle these problems is provided by the coherent potential approximation (CPA),^{3,15,19–24} particularly in its multiple scattering Korringa, Kohn, and Rostoker (KKR)^{25,26} implementation.^{27–29} The theory operates by examining the actual physical system in terms of a computationally more amenable effective medium, which is determined self-consistently for each energy so as to best incorporate average disorder effects while still restoring the approximated validity of Bloch's theorem.¹ This description has been shown to satisfy a strict set of theoretical requirements,² related to the convergence and analyticity of a proper solution:^{30–33} it recovers the exact results in all the appropriate limits^{2,4,34} and it provides a highly accurate single-site representation of a realistic system^{20–24} with qualitative, systematic improvements over cruder models of disorder^{2,35–38} at a reasonable increase in computational demands.^{2,39}

On the other hand, reliance on concentration alone to model the average presence of different chemical or magnetic species cannot account for possible higher-order aspects of their actual distribution, as normally found in a real sample for bulk^{40–42}

and surfaces.^{43–45} Local atomic substitutions, in fact, typically extend their effect up to an extended length scale, which may or may not correspond to that of crystalline periodicity, or other forms of long-range order (LRO) in a sample.

Attempts to improve the original single-site CPA formulation to also describe such short-range order (SRO) or intermediate disorder scenarios have prompted a large body of theoretical efforts. It is beside the scope of this contribution to extensively review pre-existing suggestions, in their respective merits and shortcomings. A detailed review has recently been proposed for instance by Rowlands.⁴⁶ Here, we adopt instead the pragmatic approach of identifying in previous proposals a basic dichotomy, which places on the one side developments to include the case of complex unit cell materials, where some forms of disorder coexist with undisturbed periodicity on the other sublattices,⁴⁷ and on the other side, those attempts to explicitly re-insert local higher-order corrections in the original theory for single sublattice systems, thus going beyond the first step of single-site only results.³³ This complementary outlook will inspire and guide the basic suggestion of our work towards a combined solution.

Along the latter line of research, the nonlocal coherent potential approximation (NLCPA) has been recently developed, based on insights provided by the dynamical cluster approximation,⁴⁸ in a quest to provide an efficient first-principles treatment with such desirable features as those already highlighted, for instance, in the travelling cluster approximation (TCA).³² Going beyond model Hamiltonian studies,^{46,49–52} this relatively new method has shown its capability to describe SRO effects also when it is reimplemented within a completely self-consistent DFT-KKR framework for real materials.^{51,53,54}

However, this technique inherits from its initial derivation a practical restriction to simple, one atom per unit cell lattices in *Strukturbericht* A_h (SC), A2 (bcc), or A1 (fcc) structures. In this paper, we re-examine the foundations of such approach and proceed to generalize it to also include the case of a complex unit cell and multiple sublattices scenarios in arbitrary geometries. Following a preliminary examination in

the context of a basic model Hamiltonian application,⁵⁵ this work considers, in particular, the problem from the perspective of multiple scattering calculations for actual materials. Many relevant examples for such a development spring to mind including high- T_c superconductors, multiferroics, candidate compounds for hydrogen storage, etc. To illustrate some of the effects that the new method can describe, we presently apply it to the well-known example of zirconia stabilized in the cubic phase by doping with yttria.

The paper is organized as follows. The essential aspects of the original CPA method are briefly reviewed, and its single-site limitations are tracked down, in particular, to the step where the conditional averages over a variety of local realizations of lattice occupations are evaluated. Our analysis points out how higher-order corrections, already quantified by Mills *et al.* for model Hamiltonians in the traveling cluster approximation (TCA),³³ are missed out in the original CPA theory. We recap from a similar angle the alternative strategy to reinstate these terms, adopted by the original DCA/NLCPA (see Sec. II), and the independent generalization of the single-site CPA, proposed instead by Pindor *et al.*⁴⁷ to describe complex unit cell cases without SRO (MSCPA, Sec. II C). Finally, we present our unified solution for the treatment of both aspects of the problem over the whole spectrum of LRO and SRO scenarios in complex lattice materials, as a formal merger of the MSCPA and NLCPA in the context of alternative extension attempts (see Sec. III).^{24,32–34,56–65}

This multi-sub-lattice, nonlocal version of the theory (MSNLCPA) is first put to the test by artificially examining the A_2 (A_1) disordered $\text{Cu}_{1-c}\text{Zn}_c$ metallic alloy as an example of a multi-sub-lattice B_2 (L_1) material, demonstrating the full equivalence of our MSNLCPA results to those of the original NLCPA⁵¹ (see Sec. III C) in representative SRO regimes where both treatments are possible.

We then demonstrate the new functionality of the method with an application to the example of cubic zirconia, where the study of multiatomic doping effects is contrasted for clarity and completeness with the outcome from standard supercell and original MSCPA treatments (see Sec. III D). The main aspects of these developments are finally summarized in Sec. IV.

II. EFFECTIVE MEDIUM STUDIES OF DISORDERED SYSTEMS

We briefly review the basic ideas of our work by referring to a generic binary alloy in the form $A_{1-c}B_c$. Our interest lies with observables that involve a statistically significant number of randomly occupied lattice sites, over which averaged properties are assessed. Typical experimental techniques include those of photoemission and nuclear magnetic resonance spectroscopies, electrical and optical transport, estimates of magnetic and compositional transition temperatures, and so on.

In all these cases, it is a great number of configurations of atomic species A and B within different local arrangements that give rise to the aggregated, observable result. An exhaustive evaluation of the ensemble of microscopic features is, in general, both unmanageable and beyond measurable resolution.^{6,66}

We approach the computational challenge posed by these scenarios by replacing instead the original problem with

an effective medium description. This represents a further step of abstraction in the general context of treating real materials by means of density functional theory (DFT), in which Kohn-Sham quasiparticles are evaluated starting from an approximation of the actual many-body potential generated by all charges, in the specific arrangement of various atomic sites on a lattice.

In a multiple scattering solution to such problem, these “scatterers” are decoupled in the effect produced by local interactions and the effect of the global spatial distribution. Such separation is used to efficiently determine the electronic propagator $\mathcal{G}(\mathbf{k}, \epsilon)$ and its various observables such as, in particular, the electronic charge density. This provides the necessary input for further iteration of the Kohn-Sham scheme until convergence is achieved.⁶⁷

The core of this effective medium scheme predates, in practice, the modern success of DFT,^{27,34} but has been found to be particularly productive for realistic applications when combined with this basic approach to the electronic many-body problem. When some form of disorder disrupts the periodicity of the scattering potentials arrangement over the various lattice sites, the CPA applies to the above first-principles method the additional demand that the system Green function should self-consistently reproduce the average properties of the actual material when considered over a large enough portion of the bulk. We briefly review the basics of this technique to also highlight one of its specific limitations before examining some suggested amendments.

A. The coherent potential approximation and its single-site nature

In the original derivation by Faulkner and Stocks,⁶⁸ an approximation for the ensemble-averaged propagator $\bar{\mathcal{G}}(\mathbf{k}, \epsilon)$ is offered in terms of an effective medium scattering path operator $\bar{\tau}(\epsilon)$. This mathematical object implicitly contains all specific properties of the system (regular and irregular forms for the wave function solution at the individual scatterer origin, Z and J , are still also needed to fully express the Green function), and is efficiently and conveniently represented in a spherical harmonics and lattice site basis.⁶⁹ We represent here matrices in each such index pair by underlining and denote the approximated effective medium quantities with a bar, as in $\bar{\tau}(\epsilon)$.

The CPA provides a scheme to obtain this quantity from the condition of no extra scattering coming on average from any embedded impurities, in the weak or strong, highly diluted or dense concentration limits, and at all energies.^{27,29,34,67} In practice, this constraint can be enforced starting for each energy ϵ from the T -matrix approximation (ATA) as an ansatz,⁷⁰ which posits for the t matrix associated with every site the average form

$$\alpha = A \quad \text{or} \quad B \Rightarrow \bar{t}(\epsilon) = (1 - c)t_A(\epsilon) + ct_B(\epsilon). \quad (1)$$

If we assume that the CPA effective medium should be on average the same on each lattice position n , we can alternatively adopt an integral representation over the Brillouin zone Ω and restrict ourselves to the finite site-diagonal part of $\bar{\tau}(\epsilon)$, given as

$$\bar{\tau}^{n,n}(\epsilon) = \frac{1}{\Omega} \int_{\Omega} d\mathbf{k} [\bar{m}(\epsilon) - \underline{G}(\mathbf{k}, \epsilon)]^{-1}, \quad (2)$$

where $\overline{m}(\epsilon) = \overline{t}^{-1}(\epsilon)$ and $\underline{G}(\mathbf{k}, \epsilon)$ represents the structure constants matrix.^{69,71,72}

A self-consistent prescription can then be set up, by requiring that a concentration weighted sum of the conditional averages over constituents in direct space should also lead to the same result, up to the desired tolerance:

$$\overline{t}^{n,n}(\epsilon) = (1 - c)\underline{t}_A^{n,n}(\epsilon) + c\underline{t}_B^{n,n}(\epsilon) = \sum_{\alpha} c_{\alpha}\underline{t}_{\alpha}^{n,n}(\epsilon), \quad (3)$$

where $\underline{t}_{\alpha}^{n,n}(\epsilon)$ describes an impurity of type α , embedded in the CPA medium at site n . This quantity⁷³ can be obtained through application of the corresponding projector:⁶⁸

$$\underline{D}_{\alpha}(\epsilon) = \{1 + \overline{t}^{n,n}(\epsilon)[\underline{m}_{\alpha}(\epsilon) - \overline{m}(\epsilon)]\}^{-1} \quad (4)$$

for $\underline{m}_{\alpha}(\epsilon) = \underline{t}_{\alpha}^{-1}(\epsilon)$, so that

$$\underline{t}_{\alpha}^{n,n}(\epsilon) = \underline{D}_{\alpha}(\epsilon)\overline{t}^{n,n}(\epsilon) \quad (5)$$

and iteration between Eqs. (2) and (3), until both prescriptions converge to the same scattering path operator $\overline{t}^{n,n}(\epsilon)$, provides the desired CPA description of any average site within the supposedly infinite bulk. The ATA idea has been, in practice, fully embraced and extended to represent here just the first half of a more accurate, self-consistent scheme.

We follow Mills *et al.*³² in calling, however, attention to a basic assumption of this approach. The conditional ensemble average of $N - 1$ randomly occupied sites has been, so far, worked out by simple factorization into N fully uncorrelated substitutions. When more than one disordered contributions are to be considered together though, a proper averaging procedure should also contain higher order terms. In the generic example of N random variables X_1, X_2, \dots, X_N , these corrections can be recursively defined in the form of cumulant averages (CA):^{21,32,66,74,75}

$$\begin{aligned} \langle X_1 \rangle &= \langle X_1 \rangle^C, \\ \langle X_1 X_2 \rangle &= \langle X_1 \rangle \langle X_2 \rangle + \langle X_1 X_2 \rangle^C, \\ \langle X_1 X_2 X_3 \rangle &= \langle X_1 \rangle \langle X_2 \rangle \langle X_3 \rangle + \langle X_1 X_2 X_3 \rangle^C \\ &\quad + \langle X_1 X_2 \rangle^C \langle X_3 \rangle^C + \langle X_2 X_3 \rangle^C \langle X_1 \rangle^C \\ &\quad + \langle X_1 X_3 \rangle^C \langle X_2 \rangle^C, \\ &\dots = \dots, \\ \langle X_1 X_2 \dots X_N \rangle &= \langle X_1 \rangle \langle X_2 \rangle \langle \dots \rangle \langle X_N \rangle + \dots, \end{aligned} \quad (6)$$

which are rigorously null only in the single-site case, and otherwise given by $\langle X_1 X_2 \rangle^C = \langle X_1 X_2 \rangle - \langle X_1 \rangle \langle X_2 \rangle$ and so forth.

In the present context, these terms reflect the influence that placement of an impurity α on site n exercises on its neighbors.⁶⁸ In a SRO regime, such an impact decays over a smaller distance than the size of the bulk and does not correspond to the effective medium periodicity, implicitly assumed in Eq. (2). Significant effects can, however, arise that are missed in the cruder single-site factorization of the original CPA theory. As noted in Introduction, the problem has been early recognized⁶¹ and has been the subject of a variety of amendment proposals, a review of which lies outside the scope of this contribution.^{46,66,70}

Our approach in proposing one possible general solution to such requirements, addressing, in particular, the difficulty^{75,76} of handling the respective suitability of a formulation in either direct or reciprocal space, picks up from the nonlocal extension

of the method.⁴⁹ This can be considered as a rederivation of Jarrell's *et al.* DCA for real materials and its efficient first-principles implementations, and which we now briefly proceed to review as a better starting point in its ability to overcome the molecular CPA (MCPA) in reconciling the inclusion of SRO with the on-average translational invariance.³¹ This foundation work will also guide and inspire our further generalization attempt for complex-unit-cell materials, which carries over the DCA/NLCPA advantages even to cases where the coarse-grained lattice Fourier transforms peculiar to such theories can be practically left out (see Sec. III).

B. The nonlocal CPA solution

The NLCPA also operates within the basis of a factorized evaluation of the effective medium as outlined in Eq. (6), set up by suitably combining the contributions from different substitutional species α . In this formalism, however, these are, in fact, considered over unpartitioned clusters of $N_c \geq 1$ sites, occupied by sets $\gamma = \{\alpha_1, \alpha_2, \dots, \alpha_{N_c}\}$ of possibly correlated impurities. A multisite probability distribution $P(\gamma)$ generalizes the role of the single-site concentration c_{α} , which emerges as the first moment only of such a more complete description of the problem.^{75,77,78} This can, in particular, fully account for different forms of SRO over a range of length scales and a maximal cutoff range fixed by the size of the cluster. When $N_c = 1$, the method reverts to the CPA treatment from which it also inherits all the analytical features of a Herglotz solution (see Sec. III B).

It becomes, however, exact in the limit of a cluster size extending to the whole bulk, $N_c = N \rightarrow \infty$, while preserving all desired properties in the practically interesting intermediate regime, requiring only moderately large clusters.

Technically, this is accomplished through a modified version of Eqs. (2) and (3), based on an enlarged but finite matrix structure for the scattering path operator $\overline{t}(\epsilon)$. Here, a second underline denotes now a blockwise extension of the original CPA matrix into an extra pair of indices, labeling different $I, J = 1, \dots, N_c$ cluster elements in the bulk (see Fig. 1). The corresponding impurity projectors become

$$\underline{D}_{\gamma}(\epsilon) = \{1 + \overline{t}(\epsilon)[\underline{m}_{\gamma}(\epsilon) - \overline{m}(\epsilon)]\}^{-1}, \quad (7)$$

where $\underline{m}_{\gamma}(\epsilon) = \underline{t}_{\gamma}^{-1}(\epsilon)$ is a matrix, diagonal in cluster site indices, that describes the single-site scattering from atoms at sites I within an arbitrarily placed cavity,⁷⁹ and is filled according to each particular configuration γ :

$$\underline{t}_{\gamma}(\epsilon) = \underline{D}_{\gamma}(\epsilon)\overline{t}(\epsilon). \quad (8)$$

Similarly to Eq. (3), we then assume

$$\overline{t}(\epsilon) = \sum_{\gamma} P(\gamma)\underline{t}_{\gamma}(\epsilon), \quad (9)$$

or may also equivalently express the contribution of each configuration γ in terms of a cavity scattering path operator $\overline{t}^{\text{cav}}(\epsilon)$, such that⁵¹

$$\overline{t}^{\text{cav}}(\epsilon) = \overline{m}(\epsilon) - \overline{t}^{-1}(\epsilon), \quad \underline{t}_{\gamma}(\epsilon) = [\underline{m}_{\gamma}(\epsilon) - \overline{t}^{\text{cav}}(\epsilon)]^{-1}. \quad (10)$$

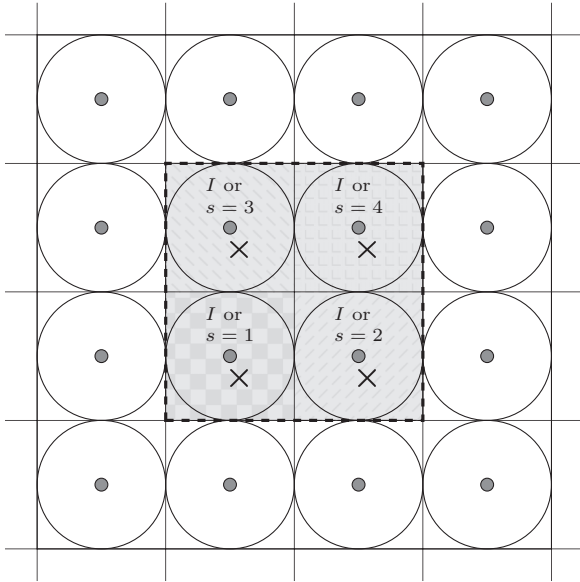


FIG. 1. Schematic depiction of a multisite cavity with $N_c = 4$ substitutional sites (darker gray). The cavity is evaluated at an arbitrary position from the effective medium (lighter gray). Various types of impurities are placed in different, possibly correlated arrangements γ , according to a multisite probability distribution $P(\gamma)$. The different labeling of distinct site occupation pertains to NLCPA (α_I index, $N_{\text{sub}} = 1$, $N_c = 4$) or MSNLCPA ($\alpha_{I,s}$ index, $N_{\text{sub}} = 4$, $N_c = 1$) descriptions, which can be equivalently deployed and lead to the same results in *ad hoc* degenerate test cases (see text).

Care is needed when extending Eq. (2) in reciprocal space, to correctly describe a finite cluster, which is still representative for the whole bulk. Jarrell *et al.*⁴⁸ and, subsequently, Rowlands *et al.*⁴⁹ have shown how this can be accomplished through a partitioning of the original Brillouin zone domain of integration Ω , which remains respectful of the underlying lattice symmetries. This is now coarse grained into N_c tiles around a discrete set of cluster momenta \mathbf{K}_n , which remain defined only up to an arbitrary phase factor, further discussed below.⁵²

The corresponding scattering path operator is hence obtained in the modified form:

$$\begin{aligned} \bar{\underline{\tau}}(\mathbf{K}_n, \epsilon) &= \frac{N_c}{\Omega} \int_{\Omega_{\mathbf{K}_n}} d\mathbf{k} [\bar{\underline{\tau}}^{-1}(\epsilon) - \underline{\delta G}(\mathbf{K}_n, \epsilon) - \underline{G}(\mathbf{k}, \epsilon)]^{-1} \\ &= \frac{1}{\Omega_{\mathbf{K}_n}} \int_{\Omega_{\mathbf{K}_n}} d\mathbf{k} [\bar{\underline{m}}(\mathbf{K}_n, \epsilon) - \underline{G}(\mathbf{k}, \epsilon)]^{-1}, \end{aligned} \quad (11)$$

where $\Omega_{\mathbf{K}_n}$ stands for the integration volume of each of the N_c tiles, defined so as to preserve on-average translational invariance in a distinctive feature for this family of theories.^{46,48} SRO corrections $\underline{\delta G}(\mathbf{K}_n, \epsilon)$ for each cluster momenta are, in particular, now made to appear and can be conveniently collected into the now \mathbf{K}_n -dependent $\bar{\underline{m}}(\mathbf{K}_n, \epsilon)$ construct of Eq. (11), together with the original $\bar{\underline{\tau}}^{-1}(\epsilon)$.

In practice, the algorithm begins again from a blockwise expression of the original ATA ansatz of Eq. (1), initially without these extra terms. It iterates between the results of Eqs. (9) and (11) through the coupled set of lattice Fourier

transforms:⁶⁶

$$\begin{aligned} \bar{\underline{\tau}}(\mathbf{K}_n, \epsilon) &= FT[\bar{\underline{\tau}}^{IJ}(\epsilon)] = \sum_J \bar{\underline{\tau}}^{IJ}(\epsilon) e^{-i\mathbf{K}_n \cdot (\mathbf{R}_I - \mathbf{R}_J)}, \\ \bar{\underline{\tau}}^{IJ}(\epsilon) &= FT^{-1}[\bar{\underline{\tau}}(\mathbf{K}_n, \epsilon)] = \frac{1}{N_c} \sum_{\mathbf{K}_n} \bar{\underline{\tau}}(\mathbf{K}_n, \epsilon) e^{+i\mathbf{K}_n \cdot (\mathbf{R}_I - \mathbf{R}_J)}, \end{aligned} \quad (12)$$

until satisfactory convergence to the same effective medium description is achieved. Here, \mathbf{R}_I denotes the position of a site within the embedded cluster, and the Brillouin zone tile centers \mathbf{K}_n are related to these vectors such that $\frac{1}{N_c} \sum_n e^{i\mathbf{K}_n \cdot (\mathbf{R}_I - \mathbf{R}_J)} = \delta_{I,J}$, so that contiguous substitutional sites are in practice examined in direct space.⁴⁹

The tiling procedure places, in fact, some constraints on the allowed sets of such N_c calculation parameters.⁴⁸ To this date, the technique has been developed only for simple lattices with just one crystallographic position per unit cell, in the case of SC, bcc, and fcc geometries.⁴⁹ Furthermore, this coarse-graining of the Brillouin zone leads to discontinuities in the \mathbf{k} -dependent integrand of Eq. (12) whenever tile boundaries are crossed.^{52,53} We note here, however, a recent proposal in the spirit of the original suggestion by Freed *et al.*^{31,62} to overcome such limitations through an additional averaging step over various phase choices, so as to reobtain a smooth, if approximated, \mathbf{k} dependence over the whole domain Ω .⁴⁶

Before proceeding to develop the multi-sub-lattice generalization of this KKR-NLCPA approach, we shall now briefly recall for clarity also the complementary extension of the single-site CPA for complex lattices, as a second foundation for our present work.

C. The multi-sub-lattice CPA for complex lattices in arbitrary geometries

We consider here the extension of the single-site CPA proposed by Pindor *et al.* for multiple sublattices compounds (MSCPA).⁴⁷ This theory is designed to cover cases of “periodic disorder,” where a material with $s = 1, 2, \dots, N_{\text{sub}}$ crystallographic positions in the unit cell may randomly host more than one atomic species per site. A prototype $N_{\text{sub}} = 2$ example can be given by the $\alpha_1 = A$ or B , $\alpha_2 = C$ or D abstract compound, in the general formula $(A_{1-c_1}, B_{c_1}), (C_{1-c_2}, D_{c_2})$.

In this case, the reciprocal space prescription for the site-diagonal scattering path operator of Eq. (2) becomes⁴⁷

$$\begin{aligned} \bar{\underline{\tau}}_{s,s'}(\epsilon) &= \frac{1}{\Omega} \int d\mathbf{k} [\bar{\underline{\tau}}^{-1}(\epsilon) - \underline{G}(\mathbf{k}, \epsilon)]_{s,s'}^{-1} \delta_{ss'} \\ &= \frac{1}{\Omega} \int d\mathbf{k} [\bar{\underline{m}}(\epsilon) - \underline{G}(\mathbf{k}, \epsilon)]_{s,s'}^{-1} \delta_{ss'} = \bar{\underline{\tau}}_s(\epsilon), \end{aligned} \quad (13)$$

where $\bar{\underline{\tau}}^{-1}(\epsilon)$ is the block-diagonal matrix with elements $\bar{\underline{\tau}}_s \delta_{s,s'}$ in sublattice space, and now $\underline{G}(\mathbf{k}, \epsilon)$ describes the structure constants for the free-electron propagation in the complex lattice.¹⁸ The self-consistent determination of the effective medium starts once again from the ATA ansatz of Eq. (1), modified to have $\bar{\underline{\tau}}_1(\epsilon) = (1 - c_1)\underline{\mathcal{L}}_A(\epsilon) + c_1\underline{\mathcal{L}}_B(\epsilon)$ and $\bar{\underline{\tau}}_2(\epsilon) = (1 - c_2)\underline{\mathcal{L}}_C(\epsilon) + c_2\underline{\mathcal{L}}_D(\epsilon)$ in this generic example of a binary alloy with only two sublattices.

This prescription is complemented by also considering the problem in direct space:⁴⁷

$$\bar{\tau}_1(\epsilon) = (1 - c_1)\tau_A^1(\epsilon) + c_1\tau_B^1(\epsilon), \quad (14)$$

$$\bar{\tau}_2(\epsilon) = (1 - c_2)\tau_C^2(\epsilon) + c_2\tau_D^2(\epsilon), \quad (15)$$

with contributions from the different impurities that may be found on each sublattice through the projectors

$$\underline{D}_{\alpha_s}(\epsilon) = \{1 + \bar{\tau}^s(\epsilon)[\underline{m}_{\alpha_s}(\epsilon) - \bar{m}_s(\epsilon)]\}^{-1}, \quad (16)$$

so that, in general,

$$\tau_{\alpha_s}^s(\epsilon) = \underline{D}_{\alpha_s}(\epsilon)\bar{\tau}^s(\epsilon). \quad (17)$$

We note that the formulation remains sublattice block-diagonal at all steps, despite the complete $N_{\text{sub}} \times N_{\text{sub}}$ block matrix inversion appearing in Eq. (13). When compared with the NLCPA of Eqs. (9)–(11), it can be seen to describe at most LRO or periodic disorder cases, but not the local effects from SRO, including those coupling the occupancies of the different sublattices. As expected, this development also reverts back naturally to the single-site CPA for $N_{\text{sub}} = 1$. It shares, furthermore, with the original formulation the lack of particular restrictions to specific lattice geometries, another advantage that we also wish to retain in the present generalization proposal.

III. THEORY EXTENSION

A. Merging the two treatments

Our strategy for combining respective benefits from the two theories of Secs. II B and II C will be again based on a self-consistent procedure to track multiple length scales in an extended cavity, as depicted for the NLCPA in Fig. 1. We still resort, in particular, to considering multisite substitutions governed by the probability distribution $P(\gamma)$ as a better tool than the concentration alone to describe different forms of short- and long-range ordering. This general scheme is derived from the NLCPA, and indeed, the following analysis will be based on the formal demand that the new generalized theory should recover the results from such a starting point or should go back to a plain supercell treatment in the appropriate limits (see Secs. III C and III D).

We intend to also match this extended model of disorder with assumptions similar to those underneath Eq. (13), where now all terms are carefully preserved and no off-diagonal contributions in sublattice space get discarded. The resulting richer description of the effective medium contains additional nondiagonal t -matrix terms $\bar{t}_{s,s'}(\epsilon)$, similar to the $\bar{t}_{IJ}(\epsilon)$ contributions in the original NLCPA.⁴⁹ When both developments are combined, the scattering path operator is also enlarged to ultimately obtain a matrix $\bar{\tau}(\epsilon)$ now labeled in general by the triplet of angular momentum (tile and sublattice indices). Relativistic extensions to further account for the spin degree of freedom are of course also possible.⁵⁴

This allows the formalism to track the effects of possibly correlated substitutions over $N_{\text{cutoff}} = N_c \times N_{\text{sub}}$ elements' length scales, or set of distances within the cavity of contiguous lattice sites, where different impurities can be hosted. Special

care must, however, be given to the important role now played by the off-diagonal blocks of the integrand from Eq. (13).

We consider here for simplicity an $N_c = 1$ example. The general expression for the extended scattering path operator $\bar{\tau}_{s,s'}(\epsilon)$ can be written as

$$\bar{\tau}_{s,s'}(\epsilon) = \frac{1}{\Omega} \int_{\Omega} d\mathbf{k} [\bar{m}(\epsilon) - \underline{\tilde{G}}(\mathbf{k}, \epsilon)]_{ss'}^{-1} \quad (18)$$

for $\bar{m}(\epsilon) = \bar{t}^{-1}(\epsilon)$ given, at first, by simple adaptation of the usual ATA prescription.

The term $\underline{\tilde{G}}(\mathbf{k}, \epsilon)$ denotes now, however, modified structure constant matrix blocks $\underline{\tilde{G}}_{s,s'}(\mathbf{k}, \epsilon)$, obtained from the original one by considering the extra sublattice-dependent phase modifier:

$$\underline{\tilde{G}}_{s,s'}(\mathbf{k}, \epsilon) = \underline{G}_{s,s'}(\mathbf{k}, \epsilon) e^{-i\mathbf{k} \cdot (\mathbf{r}_s - \mathbf{r}_{s'})}, \quad (19)$$

which can be postulated by following Banachiewicz's theorem for the blockwise inversion of a square matrix.^{80,81} Here, \mathbf{r}_s is the origin of sublattice s within a complex unit cell, and an intuitive interpretation for the action of such correction can be simply illustrated considering the two cases of *Strukturbericht* A2 and B2 lattices.

In this latter geometry, the off-diagonal structure constant matrices $\underline{G}_{s \neq s'}^{\text{CsCl}}(\mathbf{k}, \epsilon)$ are related to the ones for a bcc case according to⁴⁷

$$\underline{G}_{1,2}^{\text{CsCl}}(\mathbf{k}, \epsilon) = [\underline{G}^{\text{bcc}}(\mathbf{k}, \epsilon) - \underline{G}_{1,1}^{\text{CsCl}}(\mathbf{k}, \epsilon)] e^{+i\mathbf{k} \cdot (\mathbf{r}_1 - \mathbf{r}_2)}. \quad (20)$$

Hence, applying Eq. (19), leads us to the following expression for the nontrivial off-diagonal blocks:

$$\begin{aligned} \underline{\tilde{G}}_{1,2}^{\text{CsCl}}(\mathbf{k}, \epsilon) &= \underline{G}_{1,2}^{\text{CsCl}}(\mathbf{k}, \epsilon) e^{-i\mathbf{k} \cdot (\mathbf{r}_1 - \mathbf{r}_2)} \\ &= \underline{G}^{\text{bcc}}(\mathbf{k}, \epsilon) - \underline{G}_{1,1}^{\text{CsCl}}(\mathbf{k}, \epsilon), \end{aligned} \quad (21)$$

where $\mathbf{r}_1 = (0, 0, 0)$ and $\mathbf{r}_2 = (1/2, 1/2, 1/2)$ are possible basis vectors for the complex unit cell of an A2 lattice.

Such cancellation of the exponential from Eq. (20) operates, in other words, by removing the sublattice-diagonal free propagation modes $\underline{G}_{11}^{\text{CsCl}}(\mathbf{k}, \epsilon) = \underline{G}_{22}^{\text{CsCl}}(\mathbf{k}, \epsilon)$ from the envelope of a generic expression for $\underline{G}_{s,s'}(\mathbf{k}, \epsilon)$, initially designed to account for both diagonal and off-diagonal hopping processes (see Fig. 2).

For the $s = s'$ terms, there is no exponential argument and the original expression of panel (a) remains unchanged. The suggested modification of Eq. (19), however, ensures that, when integrating also for the new $s \neq s'$ contributions, such blocks of the scattering path operator keep resolving well distinct length scale effects, which may be sensible to sublattice-sublattice couplings. Short-range ordering can then be set up in direct space by a straightforward combination of Eqs. (7)–(9) and (14)–(16), as detailed below.

We find thus, in general,

$$\begin{aligned} \bar{\tau}_{s,s'}(\mathbf{K}_n, \epsilon) &= \frac{N_c}{\Omega} \int_{\Omega_{\mathbf{K}_n}} d\mathbf{k} [\bar{t}(\mathbf{K}_n, \epsilon) - \underline{\tilde{G}}(\epsilon, \mathbf{k})]_{s,s'}^{-1}, \\ \bar{t}_{I,s;J,s'}(\epsilon) &= \frac{1}{N_c} \sum_{n=1}^{N_c} \bar{\tau}_{s,s'}(\mathbf{K}_n, \epsilon) e^{+i\mathbf{K}_n \cdot (\mathbf{R}_I - \mathbf{R}_J)}, \end{aligned} \quad (22)$$

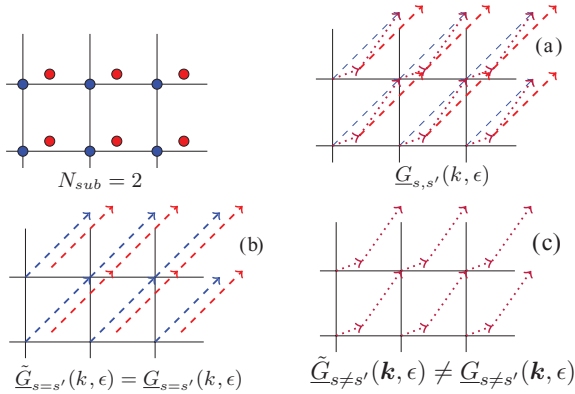


FIG. 2. (Color online) Schematic separation into distinct propagation modes for purely sublattice diagonal [$s = s'$, (b)] and off-diagonal [$s \neq s'$, (c)] free-electron hopping processes, in an $N_{\text{sub}} = 2$ sublattices case (blue and red). Different length scales can be tracked consistently with the comparable NLCPA treatment of an $N_c = 2$ simple lattice scenario, by decomposing the aggregated results of (a) into the separate contributions of (b) and (c).

as a result of applying, if required, the NLCPA lattice Fourier transforms of Eq. (12) with $\mathbf{R}_I, \mathbf{R}_J$, and \mathbf{K}_n now referring to superlattice vectors.

This larger scattering path operator $\underline{\underline{\tau}}(\epsilon)$ is again determined self-consistently by solving for contributions from different, extended cavity occupations $\gamma = \{\alpha_{1,1}, \dots, \alpha_{I,s}, \dots, \alpha_{N_c, N_{\text{sub}}}\}$, through a generalization of Eqs. (7) and (16), or the equivalent extension of Eq. (10):

$$\underline{\underline{\tau}}^{\text{cav}}(\epsilon) = \underline{\underline{t}}^{-1}(\epsilon) - \underline{\underline{\tau}}^{-1}(\epsilon), \quad \underline{\underline{\tau}}_{\gamma}(\epsilon) = [\underline{\underline{t}}_{\gamma}^{-1}(\epsilon) - \underline{\underline{\tau}}^{\text{cav}}(\epsilon)]^{-1}, \quad (23)$$

so that like in Eq. (9),

$$\underline{\underline{\tau}}(\epsilon) = \sum_{\gamma} P(\gamma) \underline{\underline{\tau}}_{\gamma}(\epsilon). \quad (24)$$

Equations (22)–(24) are then iterated self-consistently, until convergence to the same effective medium description is achieved to the desired tolerance, and other observables of interest may be computed.

B. Analytic properties of the combined solution

More generally, our strategy for the inclusion of SRO effects operates at the level of decomposing the original transition matrix \mathcal{T} given by the Dyson equation:

$$\mathcal{V}\mathcal{G} = \mathcal{T}\mathcal{G}_0, \quad (25)$$

in a context where diagonal disorder is contained by the potential term \mathcal{V} and energy dependence is omitted to ease the notation. We briefly comment on the aspects of analyticity and convergence of our modified approach, starting with some essential remarks on the general problem.

The scattering path operator τ is normally defined through adoption of the usual multiple scattering theory approximation, in which, interaction with different atoms of the lattice is assumed to take place as a sequence of distinct events, such

that $\mathcal{V} = \sum_n \mathcal{V}_n$, and therefore^{82,83}

$$\begin{aligned} \mathcal{T} &= \mathcal{V} + \mathcal{V}\mathcal{G}_0\mathcal{V} + \mathcal{V}\mathcal{G}_0\mathcal{V}\mathcal{G}_0\mathcal{V} + \dots \\ &\simeq \sum_n \mathcal{V}_n + \sum_{n,m} \mathcal{V}_n\mathcal{G}_0\mathcal{V}_m + \sum_{n,m,l} \mathcal{V}_n\mathcal{G}_0\mathcal{V}_m\mathcal{G}_0\mathcal{V}_l + \dots \\ &= \sum_{n,m} \tau_{n,m} \end{aligned} \quad (26)$$

with

$$\tau_{n,m} = t_n\delta_{nm} + \sum_{l \neq n} t_n\mathcal{G}_0\tau_{lm} = t_n\delta_{nm} + \sum_{l \neq n} \tau_{nl}\mathcal{G}_0t_m. \quad (27)$$

Under the above assumption, the CPA prescription of on-average no extra scattering from any portion of the bulk is enforced as a self-consistent version of the basic ATA condition:³⁰

$$\langle \mathcal{T} \rangle \simeq \langle t_n \rangle = 0. \quad (28)$$

This highlights the formal origin of the single-site nature of this theory. Following its very successful adoption in a variety of contexts,^{3,15–17,19,84,85} it is also at this level that many attempts to include beyond single-site effects were deployed.

Numerical⁷⁵ and subsequent analytical studies, however, quickly pointed out deep difficulties in going beyond Eq. (28). Essential features that are “automatically” implied by such a condition have been systematically examined by Yonezawa *et al.*^{2,79} and found to have crucial connections with the appropriate truncation of the diagrammatic expansion expressed by Eq. (26), fulfilling, in particular, the optical theorem⁸⁶ at various orders as discussed by Roth *et al.*^{83,87} Inconsistencies in extending the original formulation can hence easily lead to divergences or unphysical results, such as negative DOS, indeed observed in the first proposed extensions.⁷⁵

At the most basic level, the existence of a proper solution and its convergence can be proved on the simpler basis of Eq. (28).³⁰ In evaluating a Wannier space formulation of the problem, in which the role of the effective medium scattering path operator $\bar{\tau}(z)$ is fulfilled by a self-energy $\Sigma(z)$ such that $G(z) = [z - H_0 - \Sigma(z)]^{-1}$ with H_0 being the translationally invariant part of the Hamiltonian,^{31,55} the single-site term appearing above reads^{30,31,83,88}

$$t_{\epsilon_n}(z) = \frac{\epsilon_n - \Sigma(z)}{1 - [\epsilon_n - \Sigma(z)]G[z - \Sigma(z)]} \quad (29)$$

and, as elegantly illustrated by Müller-Hartmann, this is sufficient to show that a unique solution always exists for $\text{Im}(z) > 0$, through an adaptation of the fundamental theorem of algebra applied to the logarithmic derivative of such implicit definition for $\Sigma(z)$.^{2,30,89,90}

Diagrammatic approaches towards improving Eq. (28) by summing extra terms, accounting, in particular, for more complex scattering pathways involving pairs, triplets, and so on in the locator or propagator formalism, have also been proposed.⁹¹ This class of extensions implies additional complications in accounting for double counting terms, but may be counterbalanced by the ability to better abstract from a local view of the lattice, in order, for instance, to port the theory to other domains of application such as amorphous solids or liquid metals.

Our strategy fits instead within the range of “cluster-based” treatments. Here, the idea is to proceed akin to renormalization group methods, to reconstitute a formalism homologous to the original one, but applied now once more at a different scale.^{4,59,64} This is defined, in particular, by a chosen coarse-graining resolution, above which cluster quantities are still factorized out [or in the language of Eq. (6), the cumulant terms are neglected]. Within each cluster, however, the ability to simply account for SRO effects is preserved, and the general fulfillment of the desired analyticity conditions can also be simply evaluated on a matrix version of Eq. (29).⁹²

Such “molecular” modification of the CPA (MCPA) by Tsukada *et al.*^{46,70,93} has been indeed already investigated in its mathematical properties by Ducastelle *et al.*³¹ and found to be as good as the original CPA in this respect. In general, an arbitrary clustering procedure would, however, come at loss of on-average translational invariance, and while from a physical point of view such compromise can be deemed acceptable for the calculation of local quantities, such as density of states or charge,⁶¹ this would bring more severe consequences in the application to transport and other fields of linear response theory.

As demonstrated by Jarrell *et al.* at a similar level to the tight-binding description (DCA),⁴⁸ and also put to a stringent test by Lowitzer *et al.* for a fully first-principles (KKR-NLCPA) implementation of the Kubo-Greenwood formalism for the calculation of residual conductivity,^{94–96} we argue that the MSNLCPA provides a specific handling of direct and reciprocal space quantities such as to allow the above coarse-graining while also preserving on-average periodicity.⁵³ Before proceeding to illustrate other validation examples of the theory in its further extension to the case of complex-unit-cell materials (see Secs. III C and III D), we conclude this part of the discussion with a brief examination for analyticity.

The general point of view embraced by cluster-based scattering theories can be formalized by rewriting Eq. (26) as

$$\mathcal{T} = \mathcal{V}^C + \mathcal{V}^C \mathcal{G}_0^C \mathcal{V}^C + \mathcal{V}^C \mathcal{G}_0^C \mathcal{V}^C \mathcal{G}_0^C \mathcal{V}^C + \dots \simeq \sum_{cc'} \tau_{cc'}^C, \quad (30)$$

where C denotes now quantities computed for nonoverlapping clusters of lattice sites, in which the bulk is partitioned such that $\mathcal{V} = \sum_c \mathcal{V}^C$ and $\mathcal{V}^C = \{V_1, \dots, V_{N_{\text{cutoff}}}\}$.

Again, a cluster scattering path operator has been introduced above, in close analogy with the single-site Eq. (27):³¹

$$\tau_{cc'}^C = t^C \delta_{c,c'} + \sum_{c'' \neq c} t^C \mathcal{G}_0^C \tau_{cc''}^C. \quad (31)$$

(Different theories of disorder differ, in particular, in the critical details of how this quantity is in practice constructed, in order to describe the desired effective medium.)

Adopting for consistency in the following the tight-binding embodiment of the theory introduced in Eq. (29), the CPA condition reads³¹

$$\langle \mathcal{T} \rangle \simeq \langle t^C \rangle = 0, \quad (32)$$

and we need now to examine whether our underlying self-energy matrix $\underline{\Sigma}(z)$, similar in role to the effective medium

multiple scattering path operator of Eq. (22), may produce divergences for $\text{Im}(z) > 0$ in analogy to Eq. (29):

$$[\underline{\mathcal{T}}^C]_{cc'} = (V_c \delta_{c,c'} - \Sigma_{c,c'}) [\delta_{c,c'} - G_{c,c'} (V_c \delta_{c,c'} - \Sigma_{c,c'})]^{-1}. \quad (33)$$

Here, again, underlines denote square matrices in the direct space indices c, c' , analogous to the $I, s; J, s'$ convention for tiles and sublattices of Eqs. (22)–(24).

Here a critical aspect then becomes the invertibility of the matrix:

$$[\underline{D}]_{cc'} = G_{c,c'}^{-1} - V_c \delta_{c,c'} + \Sigma_{c,c'}, \quad (34)$$

specifically in view of the present off-diagonal contributions to the direct space self-energy. These represent the element of difference with respect to the original MCPA, and are indeed crucial for a proper description of SRO consistent with on-average periodicity.³¹

We can see, however, that such change does not create problems, thanks to the choice of lattice Fourier transforms (12) and the condition $\frac{1}{N_c} \sum_n e^{i\mathbf{K}_n \cdot (\mathbf{R}_I - \mathbf{R}_J)} = \delta_{I,J}$ discussed in Sec. II B. In particular, in the (MS)NLCPA formalism, the converged self-energy satisfies the idempotency relationship:

$$\underline{\Sigma}(z) = FT^{-1}\{FT[\underline{\Sigma}(z)]\}, \quad (35)$$

which can be seen, however, to imply a particular structure for the direct space matrix $\underline{\Sigma}(z)$, in which each row $2, \dots, N_{\text{cutoff}}$ is obtained from the first one as a permutation of order: $1, \dots, N_{\text{cutoff}} - 1$. This guarantees that different rows are linear independent, thus making the matrix invertible and allowing, in particular, to redeploy the rest of the demonstration as already proposed for the original scalar or matrix cases.^{30,31}

C. Validation tests

We propose that a practical approach to validating the above procedure and numerical implementation can be conceived by purposely examining some simple, one atom per unit cell lattices, taken as particular instances of multiatom per unit cell materials on a superlattice. We then require that our MSNLCPA should reproduce the original NLCPA results over all equivalent SRO scenarios, thereby resting it on the foundations of pre-existing developments in this degenerate limit.^{48,49}

A similar procedure could indeed be followed also in a preliminary, tight-binding incarnation of the theory for diagonal disorder.⁵⁵ Here, we consider instead, as a typical example of more realistic application, a Cu_{50%}Zn_{50%} alloy^{51,53} in either a bcc ($A2$) or fcc ($A1$) phases, and explore different local environment regimes with the two techniques.

A set of fully comparable structures is reported in Table I. A “degenerate” $B2$ setup, equivalently hosting either Cu or Zn atoms on both sublattices ($N_{\text{sub}} = 2, N_c = 1$), can also be examined in an NLCPA study of a $A2$ unit cell ($N_{\text{sub}} = 1, N_c = 2$). Similarly, an $L1_0$ system ($N_{\text{sub}} = 4, N_c = 1$) can also be set up to mimic the equivalent ($N_{\text{sub}} = 1, N_c = 4$) $A1$ NLCPA setup. In each case, the results should be identical.

This equivalence is confirmed for all the relevant effective medium quantities throughout the self-consistent calculation. Following Rowlands *et al.*⁵¹ we show here, in particular, the density of states at fixed stoichiometry for three very different

TABLE I. Comparable structural decompositions of the same two physical systems (first and second rows). When each sublattice is constrained to host the same atomic species with the same probabilistic distribution and over matching lattice parameters, the NLCPA and MSNLCPA are expected to coincide at the level of all effective medium quantities.

Computational budget Comparable descriptions			
Number of cavity sites	Lattice type	N_c	N_{sub}
2	bcc or A2	2	1
	CsCl or B2	1	2
4	fcc or A1	4	1
	CuAu or L1 ₀	1	4

SRO prescriptions for the two physical cases described in columns 1 and 2 of Table I (see Figs. 3 and 4).

In all cases, the SRO = 0 regime of a fully uncorrelated probability distribution $P^{\text{SRO}=0}(\boldsymbol{\gamma}) = \prod_{I=1}^{N_c} \prod_{s=1}^{N_{\text{sub}}} c[\alpha_{I,s}(\boldsymbol{\gamma})]$ corresponds to a factorized evaluation of the various elements' concentrations c throughout the cavity for $\alpha_{I,s}(\boldsymbol{\gamma})$, the atomic species found on site I,s .³⁴ As already observed in the NLCPA development, this model of disorder shows, in general, little difference from the outcome of straightforward single-site CPA calculations.

Additionally however, the extremal cases of full, local clustering^{66,97} (Warren-Cowley's nearest-neighbors order parameter SRO = +1):

$$P^{\text{SRO}=+1}(\boldsymbol{\gamma}) = c(\alpha(\boldsymbol{\gamma})) \quad \text{if } \alpha_{I,s} = \alpha \forall I,s, \quad (36)$$

or full local ordering (SRO = -1; for details see figure captions) may also be successfully compared as well as any

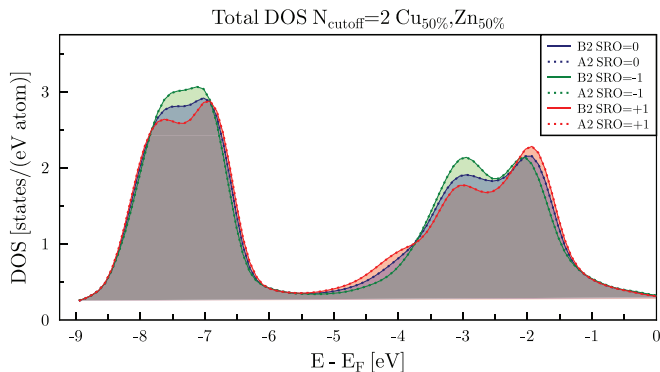


FIG. 3. (Color online) The density of states vs energy for a Cu_{50%}Zn_{50%} alloy in both a bcc and CsCl structures, evaluated for $N_{\text{sub}} \times N_c = 2$ in the three extremal short-range ordering regimes of no correlation [SRO = 0, in blue: $P(\boldsymbol{\gamma}_1 = \{\text{Cu,Cu}\}) = 25\%$, $P(\boldsymbol{\gamma}_2 = \{\text{Zn,Cu}\}) = 25\%$, $P(\boldsymbol{\gamma}_3 = \{\text{Cu,Zn}\}) = 25\%$, and $P(\boldsymbol{\gamma}_4 = \{\text{Zn,Zn}\}) = 25\%$]; complete bias towards alike neighbors [clustering, SRO = +1, in red: $P(\boldsymbol{\gamma}_1 = \{\text{Cu,Cu}\}) = 50\%$ and $P(\boldsymbol{\gamma}_4 = \{\text{Zn,Zn}\}) = 50\%$]; complete bias towards unlike neighbors [ordering, SRO = -1, in green: $P(\boldsymbol{\gamma}_2 = \{\text{Zn,Cu}\}) = 50\%$ and $P(\boldsymbol{\gamma}_3 = \{\text{Cu,Zn}\}) = 50\%$]. The NLCPA results are the dotted lines whereas the continuous line shows those of the MSNLCPA. In all three cases, the MSNLCPA CsCl results are indistinguishable from the bcc NLCPA ones.

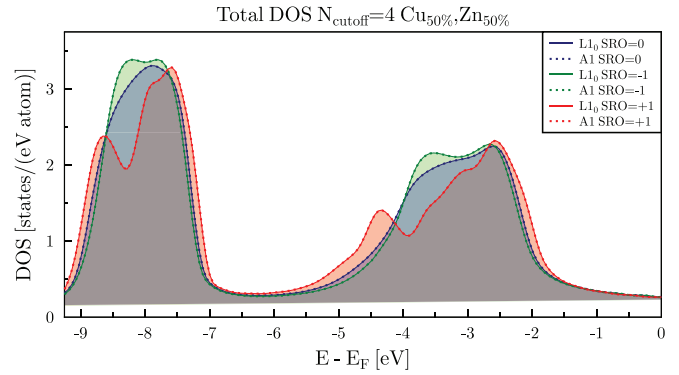


FIG. 4. (Color online) The density of states for a Cu_{50%}Zn_{50%} alloy in both an fcc and CuAu (L1₀) structure, evaluated for $N_{\text{sub}} \times N_c = 4$ in the three extremal short-range ordering regimes of no correlation [SRO = 0, in blue: $P(\boldsymbol{\gamma}_1 = \{\text{Cu,Cu,Cu,Cu}\}) = P(\boldsymbol{\gamma}_2 = \{\text{Cu,Cu,Cu,Zn}\}) = \dots = P(\boldsymbol{\gamma}_{16} = \{\text{Zn,Zn,Zn,Zn}\}) = 6.25\%$]; complete bias towards alike neighbors [clustering, SRO = +1, in red: $P(\boldsymbol{\gamma}_1 = \{\text{Cu,Cu,Cu,Cu}\}) = 50\%$ and $P(\boldsymbol{\gamma}_2 = \{\text{Zn,Zn,Zn,Zn}\}) = 50\%$]; complete bias towards unlike neighbors [ordering, SRO = -1, in green: $P(\boldsymbol{\gamma}_1 = \{\text{Cu,Zn,Cu,Zn}\}) = P(\boldsymbol{\gamma}_2 = \{\text{Zn,Cu,Zn,Cu}\}) = P(\boldsymbol{\gamma}_3 = \{\text{Zn,Zn,Cu,Cu}\}) = P(\boldsymbol{\gamma}_4 = \{\text{Zn,Cu,Cu,Zn}\}) = P(\boldsymbol{\gamma}_5 = \{\text{Cu,Cu,Zn,Zn}\}) = P(\boldsymbol{\gamma}_6 = \{\text{Cu,Zn,Zn,Cu}\}) = \simeq 16.6\%$]. The NLCPA results are the dotted lines whereas the continuous line shows those of the MSNLCPA. In all three cases, the MSNLCPA CuAu results are indistinguishable from the fcc NLCPA ones.

other types of local environments.⁴⁹ The new MSNLCPA appears to incorporate the NLCPA results as desired.

D. Yttria-stabilized zirconia

As a further application of the new method, we consider the example of zirconia, ZrO₂, stabilized into its technologically relevant cubic phase through doping with >10% mol yttria⁹⁸ Y₂O₃.

Our goal is not a thorough investigation of this material for which extensive theoretical and experimental studies are available. We adopt instead the point of view of looking specifically into further details at particular SRO effects for a relatively well-known system, to clearly illustrate some new capabilities provided by the formalism proposed in Sec. III.

In this material, experimental evidence points, in fact, towards the possible importance of this kind of phenomenology in the case, for instance, of charge transport,⁹⁹ with practical implications, for instance, in fuel cell technology. This can be the future object of a more detailed investigation based on adaptation of the method to the Kubo-Greenwood formalism,^{34,94,100} following on the footsteps of the already established suitability of the NLCPA starting point for simple-unit-cell materials.^{95,101}

We begin here our discussion by recalling some basic details about the above compound. Zirconia in the cubic phase acquires a group No. 225 structure, with superlattice generated by the fcc basis: $\mathbf{R}_1 = \{(0.0,0.5,0.5)a_{\text{lat}}, \mathbf{R}_2 = (0.5,0.0,0.5)a_{\text{lat}}, \mathbf{R}_3 = (0.5,0.5,0.0)a_{\text{lat}}\}$, $a_{\text{lat}} = 5.15 \text{ \AA}$, and a complex unit cell with sublattice origin (in cartesian coordinates): (0.0,0.0,0.0) for Zr/Y, (0.25,0.25,0.25) and (-.25,-.25,-.25) for O.

Such geometry can be stabilized by molar doping with yttria Y_2O_3 . In contrast with the substitutional scenario, typical of solid solutions such as metallic alloys, like the previously discussed $Cu_{1-c}Zn_c$ examples of Sec. III C, this process now involves multiatomic replacements in the form $(Zr_{1-c}Y_c)(O_{1-0.5c},\square_{0.5c})$ with \square to denote an oxygen vacancy.

Charge neutrality mandates in fact that for every 2 Y^{3+} cations replacing 2 Zr^{4+} , only one oxygen should be introduced in the bulk. We have in other words disorder on both the transition metal and the oxygen sublattices, at a coupled 2:1 concentrations ratio, and we intend here to examine the specific aspect of how the current formalism allows to more realistically model SRO effects between the two defects.

Previous studies^{98,102} have mimicked the doping process for a typical 33% molar Y_2O_3/ZrO_2 ratio by means of a periodically repeating SC unit cell with 12 sublattices, respectively, hosting two Y atoms, two Zr, seven O, and one vacancy.⁹⁸ This approach allows a first evaluation of the impact of yttrium inclusions at a fixed stoichiometry, which already compares favorably with ELNES experiments,⁹⁸ and also provides the advantage of a simpler computation of total energy and forces, for the practical evaluation of lattice relaxations.^{98,103}

The technique introduces, on the other hand, an unphysical form of LRO, which appears through the assumed periodicity of Y and \square replacements over the whole bulk. It also leads to increasingly more challenging calculations as the concentration is lowered, or in the case of possible co-doping scenarios. An MSCPA approach is instead exempt from the latter limitation, but suffers from the implicit assumption of complete lack of correlation between the two charged impurities. This translates into an excessively averaged out effective medium, and loss of local environment effects resolution, as further discussed in the following.

When Y^{3+} replaces Zr^{4+} , a localized negative charge is, in fact, introduced and it can be reasonably anticipated that the positive defect of a O^{2-} vacancy would preferably find itself in a contiguous region of the bulk, as opposed to being effectively “smeared out” over all the possible oxygen sites across the lattice. This aspect is, however, missing in the MSCPA description, due to lack of accounted correlations beyond the single-site perspective.

We propose to improve this picture by taking advantage of the capabilities of the modified theory discussed in Sec. III. In this example, we compare the three different treatments mentioned above, namely, standard supercell, MSCPA, and MSNLCPA with SRO, over the same $2 \times 2 \times 2$ unit cell geometry and initially for one particular concentration that appears equally amenable to each method.

The common reference starting point is the evaluation of a cavity representative of any arbitrary region of the bulk that hosts four Zr atoms, each possibly replaced by Y, and eight O atoms, each possibly replaced by the vacancy.

The supercell treatment then fixes the particular concentration ratio to compare against and provides an extra validation test for our independent implementation as a follow up to Sec. III C. From a MSCPA point of view, substitutions of two Zr atoms with Y ones correspond to a concentration of 50% for either species, and the associated replacement of an O atom out of eight with the vacancy \square gives it a concentration of 12.5%.

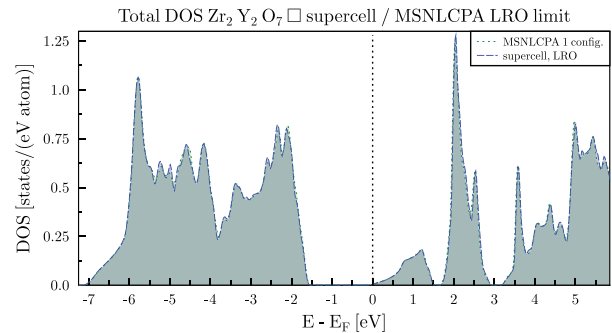


FIG. 5. (Color online) The density of states vs energy for yttria-stabilized cubic zirconia $(Zr_{1-c},Y_c)(O_{1-0.5c},\square_{0.5c})$, modeled in a degenerate MSNLCPA treatment with only one cavity arrangement allowed (dotted line, green) and in a standard supercell description (dashed line, blue). In this test for the full LRO regime, results are again indistinguishable from the alternative approach adopted as reference, as previously observed in comparisons on the $Cu_{1-c}Zn_c$ phase diagram for SRO scenarios (see Figs. 3 and 4).

The two treatments can be deemed as either the LRO or the opposite, fully uncorrelated SRO = 0 limit for the MSNLCPA extension that we wish here to further illustrate. The former corresponds in fact to the selection of a single configuration $\gamma_1^{LRO} = \{Zr,Zr,Y,Y,\square,O,O,O,O,O,O\}$ with $P(\gamma_1^{LRO}) = 100\%$, which appears in other words periodically repeating over the whole sample and is arbitrarily picked out from the complete set of $2^4 \times 2^8 = 4096$ possible arrangements of so many disordered atomic scatterers of two kinds (Zr or Y, O or \square).

The latter treatment instead implicitly considers all such contributions γ_i^{SRO} 's, each weighted by the uncorrelated probability (see Sec. III C) based on the concentrations alone.

We can indeed verify that the same DOS as in the case of a plain, CPA-free supercell can be reobtained within the new treatment (see Fig. 5), thereby completing from an opposite point of view the validation plan of Sec. III C. We then proceed to model the particular instance of yttrium/vacancy coordination here taken into consideration, by selecting from the complete, combinatorial list of γ_i 's only those specific cases where the replacement of any pairs of Zr atoms with Y (6× possible choices within four sublattices) is associated with nearby introduction of a single oxygen vacancy (8× choices), i.e., $\gamma_{i=1}^{SRO} = \{Zr,Zr,Y,Y,\square,O,O,O,O,O,O\}, \dots, \gamma_{i=48}^{SRO} = \{Y,Y,Zr,Zr,O,O,O,O,O,O,\square\}$, with $P(\gamma_i^{SRO}) = 0.0208\bar{3} \forall i = 1, \dots, 48$.

Our fully SCF-DFT⁵¹ implementation of the extended theory provides in this case complete access to the $16 \times 6 \times 8 = 768$ “polymorphous”⁴⁶ effective scattering potentials that describe interactions with each atomic species in each position of the enlarged unit cell, in addition to the dependence on the local environment as labeled by the extra index γ . We note, however, the possibility of a significant reduction in computational cost, by simplifying the above picture in terms of averages performed over equivalence classes, rather than individual elements from the set of possible cavity fillings. This point is further discussed below.

Results are initially given in Fig. 6 in terms of the total DOS from the three treatments. With this model of SRO, the

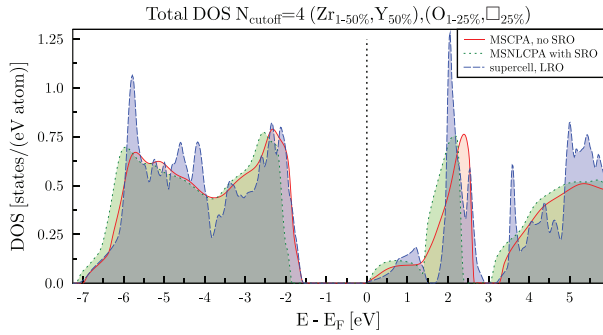


FIG. 6. (Color online) Density of states vs energy for yttria-stabilized cubic zirconia ($Zr_{1-c}Y_c$), ($O_{1-0.5c}E_{0.5c}$), modeled in a MSCPA (continuous line, red), MSNLCPA with SRO (dotted line, green) and supercell or fully LRO (dashed line, blue) treatments. Element (and configuration, where applicable) resolved contributions are given in Fig. 7.

MSNLCPA plot conveys an intermediate outcome between the relatively noisy supercell prediction, characterized by many artificially sharp features due to spurious periodicity in the repeated position of Y/Zr and \square /O substitutions, and the excessively softened MSCPA plot, with a severe smearing out of the original band structure due to the possibly excessive averaging enforced by the single-site method.

The first feature that jumps to the eye is an apparent, slight but significant shift of band gap value to a larger size, when comparing this new outcome with predictions from the two other methods. In all cases, the stoichiometry of the system is the same. While MSCPA and supercell prescribe, however, a very similar location for valence and conduction bands edges, in the new treatment, we observe some gap widening, associated with the enforced model of SRO and particularly the resulting partial sharpening of the main oxygen vacancy feature, just above E_{Fermi} (see also the last panel in Fig. 7).

This can be partially understood by considering the different effective medium structures in the three cases. In this KKR study, our Kohn-Sham quasiparticles experience an environment fully described by the set of scattering interaction potentials $V^{\text{eff}}(\mathbf{r})$, with a total energy given by the sum of kinetic, exchange, and U^{eff} contributions: $E_{\text{tot}} = T + V^{\text{eff}} = T + E_{\text{xc}} + U^{\text{eff}}$. While the second term is mainly a local aspect of the problem, related to the choice of exchange-correlation functional, the first and the third ones are directly affected by the local changes in the effective medium described above. We witness, in particular, a result of variations in the interplay between kinetic gains with easier charge delocalization, and changed costs of interactions with the other ions and electrons in the lattice. Typically, T is larger—everything else being equal—the more periodic the potential landscape looks like to the traveling quasiparticles we are investigating. U^{eff} incorporates instead various terms, but mostly relates to the more or less screened Coulomb interaction with other nuclei and electrons.

When we compare the extremal cases of MSCPA and supercell potential landscapes, we are working with a Kohn-Sham system where periodicity has been separately, self-consistently enforced within each sublattice in the unit cell. The CPA has, in particular, determined an intermediate potential between

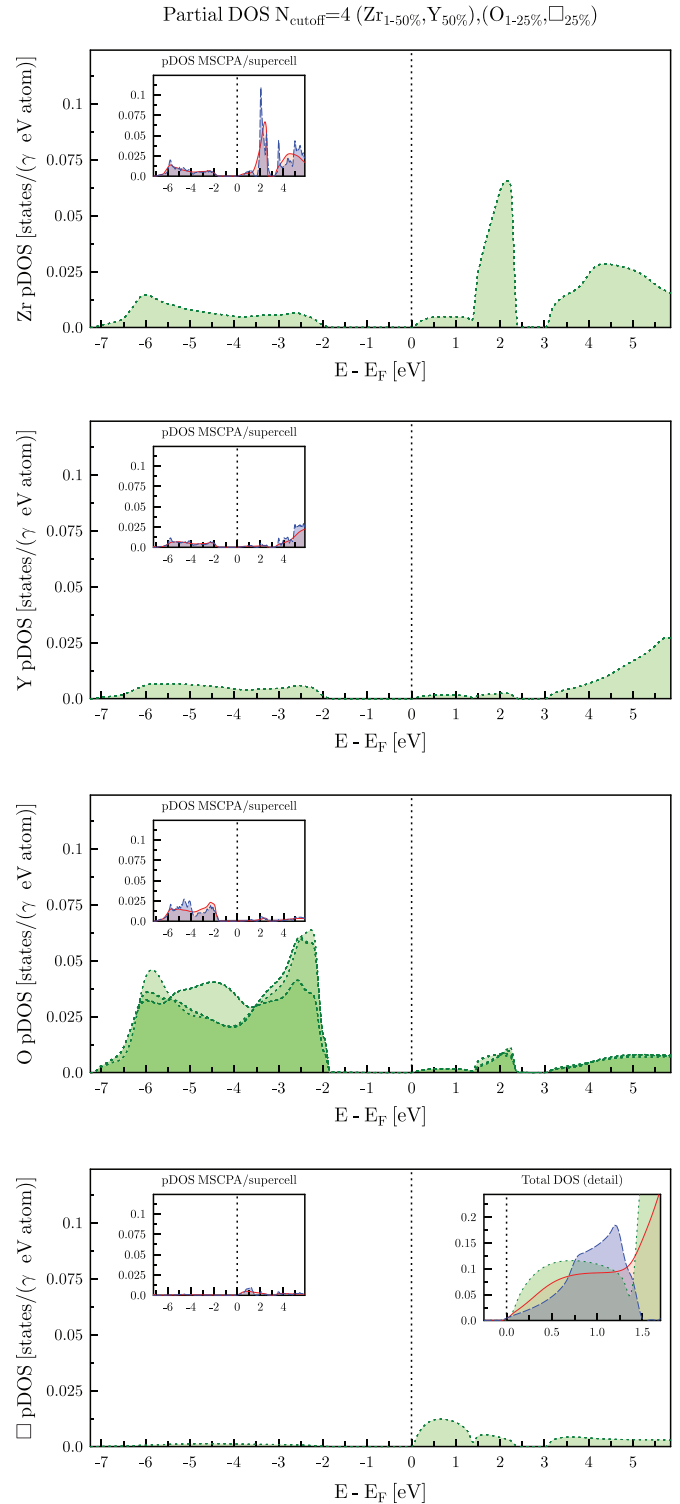


FIG. 7. (Color online) Site-, element-, and configuration-resolved DOS for yttria-stabilized cubic zirconia ($Zr_{1-c}Y_c$), ($O_{1-0.5c}\square_{0.5c}$), same notation as in Fig. 6. In all panels, the inset proposes also a comparison of the supercell and MSCPA results (left). In the last figure, the inset highlights low-lying conduction band details from the total DOS just above the Fermi level (right). For oxygen, it is evident how degeneracy with respect to local environment γ is lifted by SRO, with distinct contributions appearing as opposed to other plots where they lie on top of each other (see text).

that of pure Zr and Y, \square and O, that satisfies the request of on-average lack of extra scattering to simulate the average result over a significant subportion of the bulk that is probed by any experiment that is sensitive at once to a great many physical realizations of either Zr or Y, \square or O.

Microscopically, however, the differences between this effective potential and the one of either pure zirconium and yttrium or oxygen and vacancy are very large. When the simpler approach of a supercell calculation leaves these intrinsically unchanged, but assumes a periodic repetition over a certain LRO arrangement, a Kohn-Sham quasiparticle experiences the full impact of traveling through a rather inhomogeneous potential landscape. This translates into a small lowering of the kinetic energy in the second treatment, which is compensated, however, by a decrease in absolute magnitude of the negative U^{eff} term, with almost no change in the local-only E_{xc} term.

Our MSNLCPA model of SRO places itself in-between these two extremes. There is now no LRO repetition of completely different scattering potentials as in the supercell case, but the probabilistic view of interaction with either Zr or Y, O or \square , is not fully exempt either from local environment effects. In this study, these are formally expressed by the constraint that a single vacancy may appear in place of any oxygen atom, but only if rigorously two out of four zirconium atoms have been also replaced by yttrium, in any position within the same contiguous cavity.

This has an intuitive impact on the electrons' mobility, which cannot delocalize as much as in the perfectly periodic effective medium of the MSCPA, but are also not yet as confined in unphysical, too sharp states as in the simple supercell construction. The kinetic term of our total energy evaluation increases, approaching the value of the MSCPA scenario. The U^{eff} term is, however, also changed, resulting in a deeper valence band.

Forcing a vacancy to appear always close to two Zr/Y substitutions, we are enforcing a fair degree of coordination between effective cation/anion within the bulk. The effect can be expected to go in the direction of increased charge localization, or, in other words, shorter, less effective screening in the dominant Coulomb contribution to the U^{eff} term. A slightly larger $|U^{\text{eff}}|$ value results then in pushing down valence states relatively uniformly, with respect to either supercell or MSCPA treatments.

This takes place on top of the actual subtle changes in DOS features, which are particularly pronounced for the oxygen and vacancy contributions. The most relevant variation appears at the level of states just above the Fermi level, which undergo a significant redistribution to create a hybrid structure, in-between the MSCPA and supercell.

Our SRO results appear to inherit from the latter LRO study the nature of a relatively isolated, well resolved secondary peak that precedes the body of conduction band and remains clearly isolated from the following, mainly zirconium-like, states at 1.5–2 eV. Conversely, we can trace back to the MSCPA side an opposite tendency towards a softer shape, of hybridized band-like appearance, with smooth merging between contributions from different sublattices in the same energy range.

A complete site, element- and configuration-resolved analysis is plotted in Fig. 7. With respect to the previous discussion

of possible slight gap widening effects with SRO, the right inset of the lowest panel depicts in detail changes in the total DOS for the three treatments. We note, in particular, how a fixed stoichiometry implies that the above variations can take place only within the constraint of same unoccupied states. Correspondingly, a redefinition of the band gap, so as to be measured from the edge of the valence band to the barycenter of this first, significant feature of the conduction band, would easily reabsorb the semirigid shift discussed above.

Here, we conclude our general method discussion by simply calling attention to another aspect of the new formalism, which appears most clearly when considering, in particular, the oxygen contributions. In this particular model of SRO, results for different configurations γ are not distinguishable, with the single exception of oxygen. While for Zr/Y and the vacancy \square , all results from the complete set of 48 possible cavity fillings lie almost exactly on top of each others, the position of the vacancy appears to have a significant influence on the partial DOS from O. This can be easily understood by recalling the geometry of our $2 \times 2 \times 2$ unit cell: within the scale or SRO cutoff of the calculation, zirconium/yttrium substitutions always take place at equivalent distances, but this is not the case when it comes to the more numerous anion sublattices, which can differently host the \square defect.

The outcome is a partial lifting of electronic degeneracy across the $48 - 6 = 42$ distinct configurations, with an oxygen rather than the a vacancy on any given site. Results cluster to identify only three partial densities of states, with clearly noticeable variations.

As the general method is pushed towards larger scale calculations, a preliminary identification of such equivalence classes over which we perform direct space averages, as opposed to individual evaluation of single contributions, can be a key for enhanced scalability at no loss of accuracy, possibly on top of more approximated treatments based on importance sampling techniques.

IV. CONCLUSIONS

Most materials are affected by some degree of disorder and in many crystalline systems this affects differently various subsets of the sublattices. Often, properties nominally associated with the chemical composition of one crystallographic site can be modified by the extent and nature of disorder on another. This effect and more general cases of short-range ordering regimes can be overlooked by the original CPA, due to the single-site nature of the theory. In this paper, we briefly reexamine a theoretical extension to the original method, and suggest a strategy to efficiently perform first-principles studies over a broad class of systems by combining advantages from pre-existing techniques.

Comparison with reference results for a $\text{Cu}_{50\%}, \text{Zn}_{50\%}$ alloy in a $A2 (A1)/B2 (L1_0)$ structure could be used to provide strict validation of the new formalism against its simple unit cell implementation. As a further example of new capabilities for complex materials, the example of zirconia ZrO_2 stabilized in the cubic phase via doping with yttria Y_2O_3 has also been examined, comparing a model of SRO with predictions from the two alternative single-site CPA and supercell treatments.

ACKNOWLEDGMENTS

Financial support for parts of this work was provided by the University of Warwick Post-graduate Research Scholarship (WPRS), grants from the Deutscher Akademischer Austausch

Dienst (DAAD), and the DFG priority program SPP 1538. We wish to express our gratitude to Prof. Balazs Györfly for insightful discussions. This work is respectfully dedicated to his memory.

*amarmodo@mpi-halle.mpg.de

- ¹J. M. Ziman, *Philos. Mag.* **6**, 1013 (1961).
- ²F. Yonezawa and K. Morigaki, *Prog. Theor. Phys. Suppl.* **53**, 1 (1973).
- ³P. Soven, *Phys. Rev.* **156**, 809 (1967).
- ⁴B. Velický, S. Kirkpatrick, and H. Ehrenreich, *Phys. Rev.* **175**, 747 (1968).
- ⁵P. Soven, *Phys. Rev.* **237**, 809 (1969).
- ⁶B. L. Györfly, *Phys. Rev. B* **1**, 3290 (1970).
- ⁷S. Kirkpatrick, B. Velický, and H. Ehrenreich, *Phys. Rev. B* **1**, 3250 (1970).
- ⁸G. M. Stocks, R. W. Williams, and J. S. Faulkner, *Phys. Rev. B* **4**, 4390 (1971).
- ⁹D. Stroud and H. Ehrenreich, *Phys. Rev. B* **2**, 3197 (1970).
- ¹⁰B. Velický and K. Levin, *Phys. Rev. B* **2**, 938 (1970).
- ¹¹A. Bansil, L. Schwartz, and H. Ehrenreich, *Phys. Rev. B* **12**, 2893 (1975).
- ¹²W. Temmerman, *Phys. F* **8**, 2461 (1978).
- ¹³T. Matsubara, *Prog. Theor. Phys. Suppl.* **53**, 202 (1973).
- ¹⁴J. Staunton, B. L. Györfly, A. Pindor, G. Stocks, and H. Winter, *J. Magn. Magn. Mater.* **45**, 15 (1984).
- ¹⁵D. W. Taylor, *Phys. Rev.* **156**, 1017 (1967).
- ¹⁶N. Wakabayashi, *Phys. Rev. B* **8**, 6015 (1973).
- ¹⁷T. Kaplan and M. Mostoller, *Phys. Rev. B* **9**, 1783 (1974).
- ¹⁸J. S. Faulkner, *Phys. Rev. B* **1**, 934 (1970).
- ¹⁹Y. Onodera and Y. Toyozawa, *J. Phys. Soc. Japan* **24**, 341 (1968).
- ²⁰P. Leath, *Phys. Rev.* **171**, 725 (1968).
- ²¹F. Yonezawa, *Prog. Theor. Phys.* **40**, 734 (1968).
- ²²F. Yonezawa, *Prog. Theor. Phys.* **39**, 1076 (1968).
- ²³J. A. Blackman, D. M. Esterling, and N. F. Berk, *Phys. Rev. B* **4**, 2412 (1971).
- ²⁴H. Ueyama, *Prog. Theor. Phys.* **41**, 1375 (1969).
- ²⁵J. Koringa, *Physica* **13**, 392 (1947).
- ²⁶W. Kohn and N. Rostoker, *Phys. Rev.* **94**, 1111 (1954).
- ²⁷*Electrons in Disordered Metals and at Metallic Surfaces*, edited by P. Phariseau, B. L. Györfly, and L. Scheire, NATO ASI Series (1979).
- ²⁸W. Temmerman and Z. Szotek, *Comp. Phys. Rep.* **5**, 173 (1987).
- ²⁹B. L. Györfly, G. M. Stocks, B. Ginatempo, D. D. Johnson, D. M. Nicholson, F. J. Pinski, J. B. Staunton, H. Winter, H. Rafii-Tabar, J. B. Pendry *et al.*, *Philos. Trans. R. Soc.* **334**, 515 (1991).
- ³⁰E. Müller-Hartmann, *Solid State Commun.* **12**, 1269 (1973).
- ³¹F. Ducastelle, *J. Phys. C* **7**, 1795 (1974).
- ³²R. Mills and P. Ratanavararaksa, *Phys. Rev. B* **18**, 5291 (1978).
- ³³R. Mills, L. J. Gray, and T. Kaplan, *Phys. Rev. B* **27**, 3252 (1983).
- ³⁴A. Mookerjee, P. K. Thakur, and M. Yussouff, *J. Phys. C* **18**, 4677 (1985).
- ³⁵J. R. Klauder, *Ann. Phys.* **14**, 43 (1961).
- ³⁶J. S. Langer, *Phys. Rev.* **120**, 714 (1960).
- ³⁷F. Yonezawa, *Prog. Theor. Phys.* **3**, 357 (1964).
- ³⁸K. Levin, B. Velický, and H. Ehrenreich, *Phys. Rev. B* **2**, 1771 (1970).
- ³⁹J. Faulkner, *Int. J. Quant. Chem.* **5**, 543 (1971).
- ⁴⁰V. Capek, *Physica Status Solidi (b)* **43**, 61 (1971).
- ⁴¹A. Gonis, W. H. Butler, and G. M. Stocks, *Phys. Rev. Lett.* **50**, 1482 (1983).
- ⁴²B. L. Györfly and G. M. Stocks, *Phys. Rev. Lett.* **50**, 374 (1983).
- ⁴³N. F. Berk, *Surf. Sci.* **48**, 289 (1975).
- ⁴⁴B. Velický and J. Kudrnovský, *Surf. Sci.* **64**, 411 (1977).
- ⁴⁵L. T. Wille and P. J. Durham, *Surf. Sci.* **164**, 19 (1985).
- ⁴⁶D. A. Rowlands, *Rep. Prog. Phys.* **72**, 086501 (2009).
- ⁴⁷A. J. Pindor, W. M. Temmerman, and B. L. Györfly, *J. Phys. F* **13**, 1627 (1983).
- ⁴⁸M. Jarrell, T. Maier, C. Huscroft, and S. Moukouri, *Phys. Rev. B* **64**, 1 (2001).
- ⁴⁹D. Rowlands, J. Staunton, and B. Györfly, *Phys. Rev. B* **67**, 1 (2003).
- ⁵⁰D. Rowlands, Ph.D. thesis, University of Warwick, 2004.
- ⁵¹D. Rowlands, A. Ernst, B. Györfly, and J. Staunton, *Phys. Rev. B* **73**, 1 (2006).
- ⁵²D. Rowlands, X.-G. Zhang, and A. Gonis, *Phys. Rev. B* **78**, 115119 (2008).
- ⁵³P. Tulip, J. Staunton, D. Rowlands, B. Györfly, E. Bruno, and B. Ginatempo, *Phys. Rev. B* **73**, 1 (2006).
- ⁵⁴D. Ködderitzsch and H. Ebert, *New J. Phys.* **9**, 81 (2007).
- ⁵⁵A. Marmodoro and B. J. Staunton, *J. Phys.: Conf. Ser.* **286**, 012033 (2011).
- ⁵⁶T. Matsubara and F. Yonezawa, *Prog. Theor. Phys.* **34**, 871 (1965).
- ⁵⁷T. Matsubara and T. Kaneyoshi, *Prog. Theor. Phys.* **36**, 695 (1966).
- ⁵⁸T. Matsubara and F. Yonezawa, *Prog. Theor. Phys.* **37**, 1346 (1967).
- ⁵⁹F. Cyrot-Lackmann and F. Ducastelle, *Phys. Rev. Lett.* **27**, 429 (1971).
- ⁶⁰E.-n. Foo, H. Amar, and M. Ausloos, *Phys. Rev. B* **4**, 3350 (1971).
- ⁶¹W. H. Butler, *Phys. Lett. A* **39**, 203 (1972).
- ⁶²K. F. Freed and M. H. Cohen, *Phys. Rev. B* **3**, 3400 (1971).
- ⁶³M. Goda, *J. Phys. C* **6**, 3047 (1973).
- ⁶⁴T. P. McManus and E. Brown, *Solid State Commun.* **18**, 523 (1976).
- ⁶⁵M. Goda, *J. Phys. C* **10**, 1121 (1977).
- ⁶⁶J. M. Ziman, *Models of Disorder: the Theoretical Physics of Homogeneously Disordered Systems* (Cambridge University Press, Cambridge, UK, 1979).
- ⁶⁷D. Johnson, D. Nicholson, and F. Pinski, *Phys. Rev. Lett.* **56**, 2088 (1986).
- ⁶⁸J. Faulkner and G. Stocks, *Phys. Rev. B* **21**, 3222 (1980).
- ⁶⁹J. Zablouil, R. Hammerling, L. Szunyogh, and P. Weinberger, *Electron Scattering in Solid Matter: A Theoretical and Computational Treatise* (Springer, Berlin, 2004).
- ⁷⁰A. Gonis, *Green Functions for Ordered and Disordered Systems* (North-Holland, Amsterdam, 1992).
- ⁷¹F. Ham and B. Segall, *Phys. Rev.* **124**, 1786 (1961).
- ⁷²P. Weinberger, *Electron Scattering Theory for Ordered and Disordered Matter* (Oxford University Press, Oxford, UK, 1990).
- ⁷³B. L. Györfly and M. J. Scott, *Solid State Commun.* **9**, 613 (1971).
- ⁷⁴R. Kubo, *J. Phys. Soc. Japan* **17**, 1100 (1962).

- ⁷⁵B. G. Nickel and W. H. Butler, *Phys. Rev. Lett.* **30**, 373 (1973).
- ⁷⁶C. I. Ventura and R. A. Barrio, *Physica B* **281-282**, 855 (2000).
- ⁷⁷F. Yonezawa and T. Odagaki, *Solid State Commun.* **27**, 1199 (1978).
- ⁷⁸T. Odagaki and F. Yonezawa, *Solid State Commun.* **27**, 1203 (1978).
- ⁷⁹H. Shiba, *Prog. Theor. Phys.* **46**, 77 (1971).
- ⁸⁰J. Slechta, *J. Phys. F* **4**, 1148 (1974).
- ⁸¹J. Mašek and J. Kudrnovský, *J. Phys.: Chem. Solids* **49**, 349 (1988).
- ⁸²L. L. Foldy, *Phys. Rev.* **67**, 107 (1945).
- ⁸³L. M. Roth, *J. Phys., Colloq.* **35**, C4 (1974).
- ⁸⁴A. B. Chen, G. Weisz, and A. Sher, *Phys. Rev. B* **5**, 2897 (1972).
- ⁸⁵K. I. Wysokinski, *J. Phys. C* **2**, 291 (1978).
- ⁸⁶L. S. Rodberg and R. M. Thaler, *Introduction to the Quantum Theory of Scattering (Pure and Applied Physics)*, Vol. 26 (Academic Press, New York, 1967).
- ⁸⁷L. Schwartz and A. Bansil, *Phys. Rev. Lett.* **39**, 421 (1976).
- ⁸⁸E. Esposito, H. Ehrenreich, and C. D. Gelatt, Jr., *Phys. Rev. B* **18**, 3913 (1978).
- ⁸⁹G. Arfken and H. Weber, *Mathematical Methods for Physicists*, 5th ed. (Academic Press, New York, 2001).
- ⁹⁰E. B. Saff and A. D. Snider, *Fundamentals of Complex Analysis*, 3rd ed. (Prentice Hall, Upper Saddle River, New Jersey, 2003).
- ⁹¹Y. Ishida and F. Yonezawa, *Prog. Theor. Phys.* **49**, 731 (1973).
- ⁹²B. G. Nickel and J. A. Krumhansl, *Phys. Rev. B* **4**, 4354 (1971).
- ⁹³M. Tsukada, *J. Phys. Soc. Jpn.* **26**, 684 (1969).
- ⁹⁴W. H. Butler, *Phys. Rev. B* **31**, 3260 (1985).
- ⁹⁵P. Tulip, J. Staunton, S. Lowitzer, D. Ködderitzsch, and H. Ebert, *Phys. Rev. B* **77**, 1 (2008).
- ⁹⁶S. Lowitzer, D. Ködderitzsch, H. Ebert, P. R. Tulip, A. Marmodoro, and J. B. Staunton, *Europhys. Lett.* **92**, 37009 (2010).
- ⁹⁷F. Yndurain and L. M. Falicov, *Solid State Commun.* **17**, 1545 (1975).
- ⁹⁸S. Ostanin, A. Craven, D. McComb, D. Vlachos, A. Alavi, M. Finnis, and A. Paxton, *Phys. Rev. B* **62**, 14728 (2000).
- ⁹⁹K. Nomura, Y. Mizutani, and M. Kawai, *Solid State Ionics* **132**, 235 (2000).
- ¹⁰⁰R. Kubo, *J. Phys. Soc. Jpn.* **12**, 570 (1957).
- ¹⁰¹S. Lowitzer, Ph.D. thesis, Ludwig Maximilians Universität München, 2010.
- ¹⁰²A. Bogicevic, C. Wolverton, G. M. Crosbie, and E. B. Stechel, *Phys. Rev. B* **64**, 014106 (2001).
- ¹⁰³S. Ostanin, A. J. Craven, D. W. McComb, D. Vlachos, A. Alavi, A. T. Paxton, and M. W. Finnis, *Phys. Rev. B* **65**, 224109 (2002).